

High light extraction efficiency in bulk-GaN based volumetric violet light-emitting diodes

Aurelien David, Christophe A. Humi, Rafael I. Aldaz, Michael J. Cich, Bryan Ellis, Kevin Huang, Frank M. Steranka, and Michael R. Krames

Citation: *Applied Physics Letters* **105**, 231111 (2014); doi: 10.1063/1.4903297

View online: <http://dx.doi.org/10.1063/1.4903297>

View Table of Contents: <http://scitation.aip.org/content/aip/journal/apl/105/23?ver=pdfcov>

Published by the AIP Publishing

Articles you may be interested in

[Bulk GaN based violet light-emitting diodes with high efficiency at very high current density](#)

Appl. Phys. Lett. **101**, 223509 (2012); 10.1063/1.4769228

[Enhanced light extraction efficiency in flip-chip GaN light-emitting diodes with diffuse Ag reflector on nanotextured indium-tin oxide](#)

Appl. Phys. Lett. **93**, 021121 (2008); 10.1063/1.2953174

[Theoretical demonstration of enhancement of light extraction of flip-chip GaN light-emitting diodes with photonic crystals](#)

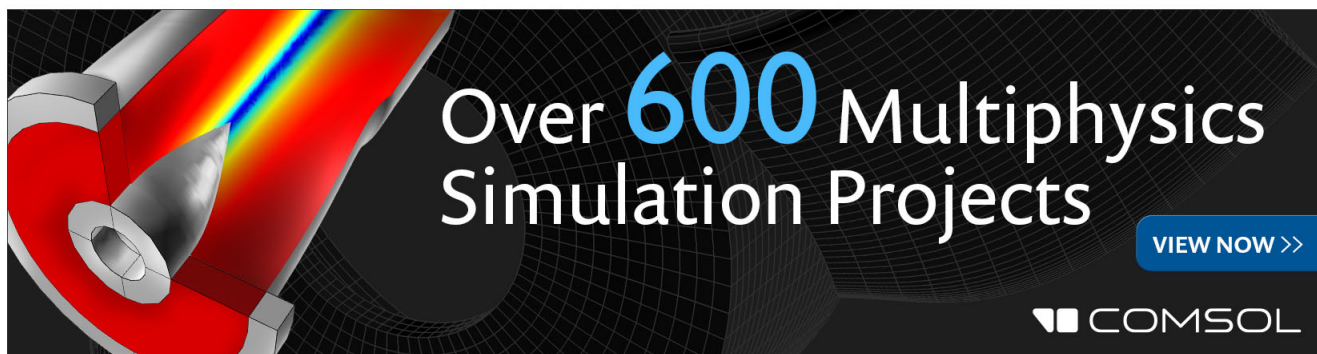
Appl. Phys. Lett. **89**, 091116 (2006); 10.1063/1.2338773

[Thermally stable and highly reflective AgAl alloy for enhancing light extraction efficiency in GaN light-emitting diodes](#)

Appl. Phys. Lett. **88**, 043507 (2006); 10.1063/1.2168264

[Increase in the extraction efficiency of GaN-based light-emitting diodes via surface roughening](#)

Appl. Phys. Lett. **84**, 855 (2004); 10.1063/1.1645992

The advertisement features a 3D simulation of a light-emitting diode (LED) structure. A red and yellow light beam is shown exiting from the device. The background is dark with a grid pattern. The text 'Over 600 Multiphysics Simulation Projects' is prominently displayed in white and blue. A blue button with the text 'VIEW NOW >>' is located in the bottom right corner. The COMSOL logo is also present in the bottom right corner.

Over 600 Multiphysics Simulation Projects

VIEW NOW >>

COMSOL

High light extraction efficiency in bulk-GaN based volumetric violet light-emitting diodes

Aurelien David,^{a)} Christophe A. Hurni, Rafael I. Aldaz, Michael J. Cich, Bryan Ellis, Kevin Huang, Frank M. Steranka, and Michael R. Krames
 Soraa Inc., 6500 Kaiser Dr., Fremont, California 94555, USA

(Received 16 October 2014; accepted 21 November 2014; published online 9 December 2014)

We report on the light extraction efficiency of *III*-Nitride violet light-emitting diodes with a volumetric flip-chip architecture. We introduce an accurate optical model to account for light extraction. We fabricate a series of devices with varying optical configurations and fit their measured performance with our model. We show the importance of second-order optical effects like photon recycling and residual surface roughness to account for data. We conclude that our devices reach an extraction efficiency of 89%. © 2014 AIP Publishing LLC. [<http://dx.doi.org/10.1063/1.4903297>]

III-Nitride light-emitting diodes (LEDs) have seen significant performance progress in past decades and are now the basis for efficient solid-state lighting. Further improvement is necessary to support adoption of this technology and the corresponding energy savings. The main figure of merit for LED efficiency is the power conversion efficiency, also called wall-plug efficiency, which is the product of the external quantum efficiency (*EQE*, i.e., the ratio of emitted photons to injected electrons) and of the electrical efficiency. The latter is controlled by the LED's forward voltage and can be improved by reducing contact and junction resistance. The *EQE* is given by

$$EQE = C_{ex} \times \eta, \quad (1)$$

where C_{ex} is the extraction efficiency and η is the internal quantum efficiency. Understanding the breakdown of these two components of *EQE* is crucial, as it provides guidance for further performance improvements. However, disentangling them is a difficult task: one can attempt to measure η directly (with experimental procedures of limited accuracy) or to predict C_{ex} from an optical model.

In principle, predicting C_{ex} is attractive because optical models can achieve high accuracy. However, this is only the case if all the relevant physics is included. In practice, few published results report on C_{ex} for high-performance LEDs.^{1–5} Often, the value of C_{ex} is predicted but is not cross-correlated with experimental data so that the accuracy of the model cannot be assessed.

In this letter, we present an advanced optical model to predict C_{ex} and demonstrate its accuracy by consistently matching the experimental performance of a series of LEDs with varying optical configurations.

We begin with a short discussion of the optical model and its implications. Standard raytracing is often employed to model C_{ex} .^{6–11} In our case, however, this is not fully warranted: we employ small-scale ($\sim 1 \mu\text{m}$) surface roughness (SR) to randomize photon trajectories,^{12–14} and ray optics do not necessarily apply in such a regime.^{4,15,16}

Rather, as discussed in Ref. 17, the optical behavior of SR can be accurately modeled in a wave-optics framework. In this approach, the scattering matrix (relating the amplitude of incoming and outgoing waves) for a textured interface is predicted by solving Maxwell's equation, and averaged over various configurations to obtain statistical trends. The study of Ref. 17 concludes that SR scattering has a non-trivial behavior, different from an ideal Lambertian diffuser. In particular, scattering depends on the angle of incidence of light as sketched in Figs. 1(a) and 1(b): near normal incidence it is mostly diffuse, but at large angle *specular reflection* dominates. Reference 17 also shows that the scattering behavior can be parametrized by a single parameter, the scattering strength f of the SR, with $f=0$ corresponding to a smooth interface and $f=1$ corresponding to maximally scattering SR.

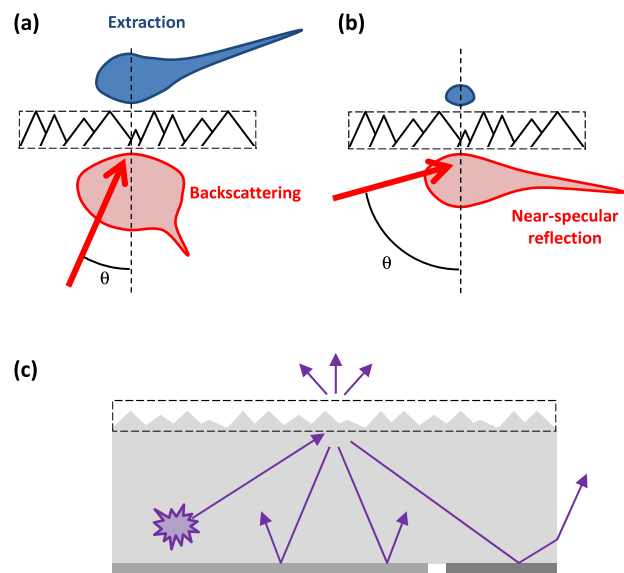


FIG. 1. (a) and (b) Scattering properties of SR. For light impinging near normal incidence, (a) scattering is split between an extracted component (blue cloud) and a mostly diffuse backscattered component (red cloud). At large incidence angle, (b) extraction is weak and backscattering becomes mostly specular. (c) Inclusion of the SR model into a raytracing model. Rays follow standard raytracing propagation; when they impinge on the SR, new scattered rays are generated according to the SR model.

^{a)}Electronic mail: adavid@soraa.com

Once the scattering matrix for SR is computed, it can be integrated into a raytracing code to generate C_{ex} predictions as shown in Fig. 1(c). A commercial code can be used; however, here we use a proprietary code for additional convenience and performance. We include various relevant optical effects: angle- and polarization-dependent reflectivity and loss for all interfaces, Fresnel reflection for smooth interfaces, accurate scattering results for SR interfaces, and the angular radiation diagram from the light-emitting region.¹⁸

As discussed in Ref. 17, our realistic SR model has important implications: in contrast to a simple model (e.g., photon gas based on Lambertian diffusion^{1,19}), it predicts that large-angle light can remain trapped in an LED for many bounces and eventually be absorbed. This effect is especially limiting in conventional thin-film LEDs¹⁷ but can be mitigated by using so-called volumetric LEDs²⁰ with a vertical-to-horizontal aspect ratio close to unity. Volumetric LEDs are enabled by the use of bulk GaN substrates. They let light escape both from the top and side surfaces, thus addressing the imperfect scattering by SR. Reference 20 predicts that, with a volumetric approach, C_{ex} can approach 90%, significantly higher than values reported for thin-film chips.

In order to validate the accuracy of the optical model, however, we must compare it to experimental results. To this effect, we put the model to a demanding experimental test: we fabricate a series of LEDs with varying optical properties and seek to fit all their measured performance consistently.

The epitaxial layers used for the LEDs are grown on low dislocation density bulk GaN substrates by metal-organic chemical vapor deposition. They emit around $\lambda = 415$ nm. All devices use similar epi wafers. We fabricate volumetric LEDs with a triangular shape and a flip-chip contact architecture. We vary the following parameters: *p*-mirror metal (low-reflectivity Ni or high-reflectivity Ag); top surface (smooth or rough); and sidewall surface (smooth or rough). Fig. 2 shows an image of a device with roughened top and sidewall surfaces. We combine all parameters in a $2 \times 2 \times 2$ factorial design.²¹ The design with Ag *p*-mirror and roughened side and top surfaces is representative of our production devices.

For each LED design, we measure the *EQE* at room temperature at a current density of 9 A cm^{-2} (corresponding to peak *EQE*), both for emission in air and in a standard encapsulant ($n_{enc} = 1.4$). Here and in the following, we use the indices *air* and *enc* for these respective values. Therefore, we obtain 14 *EQE* values to be fitted by the optical model. We note that with respect to Eq. (1), experimental *EQEs* are multiplied by an additional factor: the package efficiency (*PE*) of the package holding the die. *PE* represents the fraction of light emitted by the die which escapes from the test package; its contribution needs to be factored out to analyze results. To this effect, we carefully model light propagation from the chip into the package with raytracing. We use measured values for the reflectivities of all package interfaces in order to predict optical loss accurately. We obtain $PE = 94\%$. All the *EQE* data reported in the following are normalized by this value. Fig. 3(a) shows the experimental *EQEs*. Qualitatively, the trends are as expected: *EQE* increases with a more reflective *p*-contact and with the addition of SR.

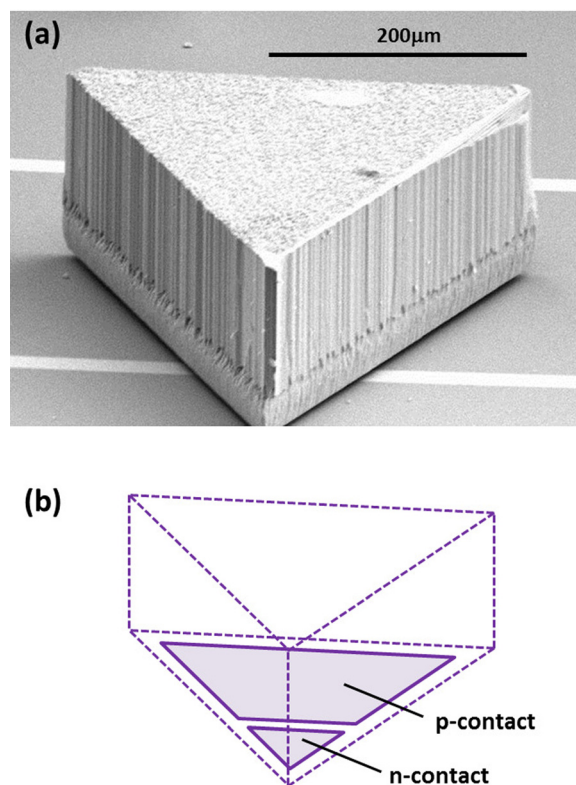


FIG. 2. (a) Scanning electron microscope image of a fabricated LED with roughened top and side surfaces. (b) Corresponding device geometry.

To better understand the data, we now introduce the so-called encapsulation gain (*EG*)

$$EG = \frac{EQE_{enc}}{EQE_{air}} = \frac{C_{ex enc}}{C_{ex air}}. \quad (2)$$

EG is an important quantity for two reasons. First, as seen in Eq. (2), η cancels out in the expression of *EG*.²² Therefore, even if η is unknown, it is possible to test an optical model by comparing the predicted and measured values of *EG*.

Second, and more importantly, *EG* serves as a proxy for optical loss in an LED. To understand this intuitively, let us consider a simplistic model where light bounces *N* times in an LED before extraction and undergoes an average single-bounce loss *L*. In this case, $C_{ex} = 1 - N \times L$ and *EG* becomes

$$EG = \frac{1 - N_{enc} \times L}{1 - N_{air} \times L}. \quad (3)$$

It can be seen from Eq. (3) that *EG* is always larger than 1 (light bounces more before extraction into air than into an encapsulant, i.e., $N_{air} > N_{enc}$). Moreover, *EG* decreases as *L* decreases, reaching an ideal value of 1 for $L = 0$ (i.e., $C_{ex} = 1$). Therefore, for a given device architecture, the value of *EG* gives insight into the amount of optical loss; low values of *EG* are desirable as they are indicative of a low-loss device. We stress that *EG* is routinely used for this purpose in the LED industry, although it seems to have found little usage in academic investigations. Although the model leading to Eq. (3) is simple, more accurate treatments result in similar trends.

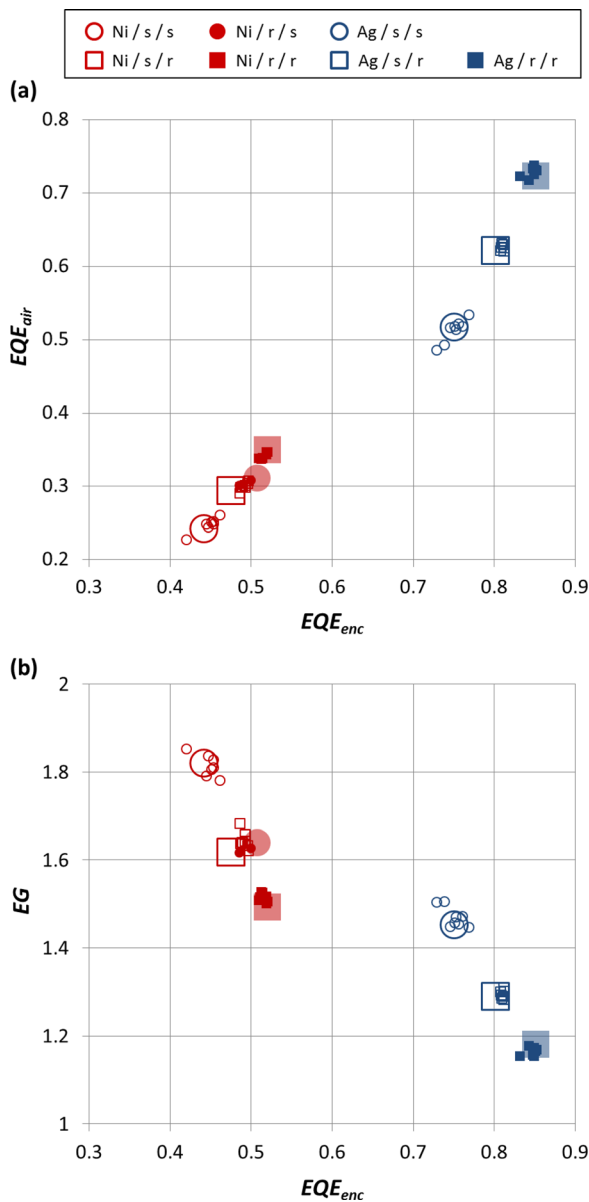


FIG. 3. Experimental and modeled performance of the LEDs. (a) The EQE_{air} in air and encapsulant and (b) re-casts the data as encapsulated EQE and encapsulation gain. The small symbols are the experimental data (one point per LED). The model results correspond to the large symbols (whose size has been adjusted to approximate the experimental spread). The legend indicates the device type: p -contact/top roughness/side roughness (s: smooth, r: roughened).

Fig. 3(b) recasts the data in terms of EQE_{enc} and EG ; this data is equivalent to that of Fig. 3(a), but the values of EG provide additional intuitive insight.

As a preliminary exercise to fitting all experimental data, let us focus on a simple device configuration: Ag p -mirror and smooth top and side interfaces. In this simple case the value of EG is easily predicted as the ratio of the extraction cones to air and epoxy, yielding $EG = n_{enc}^2 \approx 2$. This textbook value is in stark contrast to the experimental result: $EG \approx 1.45$. To explain this discrepancy, we must account for two non-trivial extraction effects.

First, photon recycling^{2,23} (PR) plays a large role in the performance of our LEDs. Indeed, we employ thick light-emitting layers to mitigate droop; this entails significant single-pass absorption, as shown in Fig. 4. Our devices also

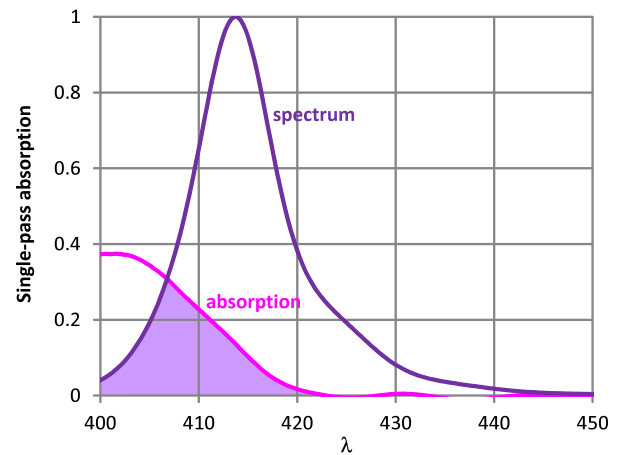


FIG. 4. Single-pass absorption through the light-emitting layers. The normalized emission spectrum, also shown, has significant overlap with the absorption spectrum.

have a high η so that much of the absorbed light can be re-emitted, leading to PR. This effect boosts C_{ex} in all devices, and is most pronounced for smooth devices (where much light is trapped and prone to re-absorption). PR can be included in the optical model as follows:

$$C_{ex}^* = \frac{C_{ex}}{1 - \eta A}, \quad (4)$$

where C_{ex} is the extraction without PR, C_{ex}^* is the extraction with PR, and A is the net absorption by the light-emitting layers. C_{ex} and A are computed by the optical model, then Eq. (4) yields C_{ex}^* for a given value of η . By including PR in the model, we find that the predicted EG for smooth devices drops from 2 to 1.68. This is closer to the experimental data, albeit still too high.

The second factor which contributes to lowering EG is unintentional surface roughness on the sidewalls of the LEDs. Indeed, some amount of SR is induced by the die singulation process even when a smooth surface is sought. Therefore, we must include a non-zero value for sidewall roughness f_{side}^{smooth} . Even though this SR is weak, it has a strong impact on EG : a scattering strength of $f_{side}^{smooth} = 2.5\%$ is sufficient to fit the experimental results. Fig. 5 illustrates how the experimental data for the smooth LEDs is well fitted by including PR and unintentional SR; both EG and EQE_{enc} are well fitted at the same time. Note that the top surface roughness is kept at a value of zero, as this surface can be made perfectly smooth.

This discussion illustrates that second-order effects (PR and unintentional SR) play a large role even in a seemingly simple device geometry. This has implications in many practical cases. For instance, high EQE is sometimes investigated in volumetric devices with no intentional extraction features.^{9,24} In such devices, ignoring second-order effects can lead to underestimating C_{ex} by 15%–25%—a large difference which also has bearing on the estimation of η . Likewise, in test structures with a planar device geometry,^{25,26} second-order effects can significantly modify the predicted value of C_{ex} .

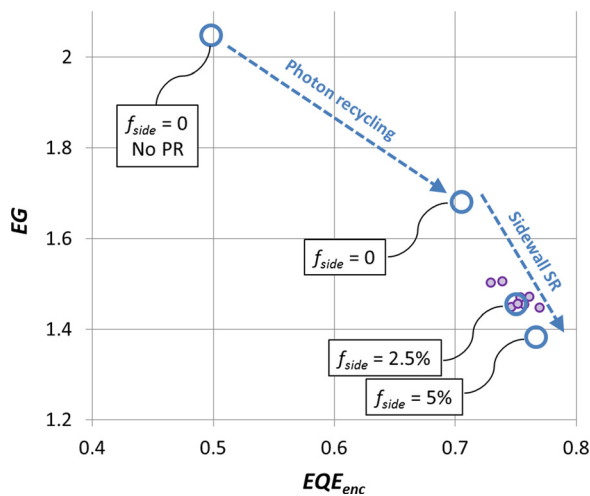


FIG. 5. Results for smooth die with Ag p -contact. Violet dots: experimental data. Blue circles: model. Inclusion of PR and sidewall SR is necessary to fit the data. The labels indicate the model results for various values of the sidewall roughness parameter f_{side}^{smooth} . A modest value is sufficient to significantly lower EG.

Now that this simplest device configuration is understood, we seek to fit all the experimental data. Our model only has three free parameters: η and the scattering strengths f_{top} and f_{side} for the intentionally-roughened top and side interfaces. We use the same three parameters to fit all device results. After optimizing these parameters, we obtain the predictions shown in Fig. 3: they are in excellent agreement with the experimental data. Since we are fitting 14 measurements, the problem is significantly over-determined; in other words, it is by no means trivial to fit all data with the same parameters at once. Therefore, the agreement shown in Fig. 3 is a clear indication of the accuracy of the model.

As an outcome of the fitting procedure, we obtain $\eta = 95\%$ and $C_{ex} = 89\%$ for the best devices (Ag p -contact and roughened surfaces). These values are the highest reported for commercial LEDs in any material system and warrant our volumetric chip approach. In an upcoming publication,²⁷ we will demonstrate how this chip architecture yields very high overall efficiency. Additionally, the high extraction presented here is obtained for violet devices ($\lambda = 415$ nm), for which optical losses are relatively high. In the case of blue devices ($\lambda = 450$ nm) where optical losses are lower, our model predicts that a value as high as $C_{ex} = 95\%$ could be achieved. Both of these values are very close to the practical limit in realistic devices.

In conclusion, we presented a light extraction model based on an accurate treatment of surface roughness. We used it to simultaneously fit the performance of a series of LEDs with varying optical designs, thus validating the model's accuracy. We introduced encapsulation gain as an important quantity to interpret optical performance. We showed that non-trivial effects such as photon recycling and unintentional roughness could largely impact the performance of LEDs. We demonstrated a state-of-the-art light extraction of 89% in volumetric violet LEDs. In general, we believe that such accurate optical modeling has broad applicability and is of importance to guide research in optoelectronic devices.

- ¹I. Schnitzer, E. Yablonovitch, C. Caneau, T. J. Gmitter, and A. Scherer, "30% External quantum efficiency from surface textured, thin-film light-emitting-diodes," *Appl. Phys. Lett.* **63**, 2174–2176 (1993).
- ²I. Schnitzer, E. Yablonovitch, C. Caneau, and T. J. Gmitter, "Ultrahigh spontaneous emission quantum efficiency, 99.7% internally and 72% externally, from AlGaAs/GaAs/AlGaAs double heterostructures," *Appl. Phys. Lett.* **62**, 131–133 (1993).
- ³M. Boroditsky and E. Yablonovitch, "Light-emitting-diode extraction efficiency," in *Proc. SPIE* **3002**, 119–122 (1997).
- ⁴R. Windisch, C. Rooman, B. Dutta, A. Knobloch, G. Borghs, G. H. Dohler, and P. Heremans, "Light-extraction mechanisms in high-efficiency surface-textured light-emitting diodes," *IEEE J. Sel. Top. Quantum Electron.* **8**, 248–255 (2002).
- ⁵M. R. Krames, O. B. Shchekin, R. Mueller-Mach, G. O. Mueller, L. Zhou, G. Harbers, and M. G. Craford, "Status and future of high-power light-emitting diodes for solid-state lighting," *J. Disp. Technol.* **3**, 160–175 (2007).
- ⁶S. J. Lee, "Analysis of light-emitting diodes by Monte Carlo photon simulation," *Appl. Opt.* **40**, 1427–1437 (2001).
- ⁷T.-X. Lee, K. Gao, W.-T. Chien, and C.-C. Sun, "Light extraction analysis of GaN-based light-emitting diodes with surface texture and/or patterned substrate," *Opt. Express* **15**, 6670–6676 (2007).
- ⁸Y.-K. Ee, P. Kumnorkaew, R. A. Arif, H. Tong, J. F. Gilchrist, and N. Tansu, "Light extraction efficiency enhancement of InGaN quantum wells light-emitting diodes with polydimethylsiloxane concave microstructures," *Opt. Express* **17**, 13747–13757 (2009).
- ⁹S. E. Brinkley, C. L. Keraly, J. Sonoda, C. Weisbuch, J. S. Speck, S. Nakamura, and S. P. DenBaars, "Chip shaping for light extraction enhancement of bulk c-plane light-emitting diodes," *Appl. Phys. Express* **5**, 032104 (2012).
- ¹⁰M. Shatalov, W. Sun, A. Lunev, X. Hu, A. Dobrinsky, Y. Bilenko, J. Yang, M. Shur, R. Gaska, and C. Moe, "AlGaIn deep-ultraviolet light-emitting diodes with external quantum efficiency above 10%," *Appl. Phys. Express* **5**, 082101 (2012).
- ¹¹C. Lalau-Keraly, L. Kuritzky, M. Cochet, and C. Weisbuch, "Light extraction efficiency part a. ray tracing for light extraction efficiency (LEE) modeling in nitride LEDs," in *III-Nitride Based Light Emitting Diodes and Applications* (Springer, 2013), pp. 231–269.
- ¹²T. Fujii, A. David, C. Schwach, P. M. Pattison, R. Sharma, K. Fujito, T. Margalith, S. P. Denbaars, C. Weisbuch, and S. Nakamura, "Micro cavity effect in GaN-based light-emitting diodes formed by laser lift-off and etch-back technique," *Jpn. J. Appl. Phys., Part 2* **43**, L411–L413 (2004).
- ¹³T. Fujii, A. David, Y. Gao, M. Iza, S. P. DenBaars, E. L. Hu, C. Weisbuch, and S. Nakamura, "Cone-shaped surface GaN-based light-emitting diodes," *Phys. Status Solidi C* **2**, 2836–2840 (2005).
- ¹⁴O. B. Shchekin, J. E. Epler, T. A. Trottier, T. Margalith, D. A. Steigerwald, M. O. Holcomb, P. S. Martin, and M. R. Krames, "High performance thin-film flip-chip InGaIn-GaN light-emitting diodes," *Appl. Phys. Lett.* **89**, 071109 (2006).
- ¹⁵R. Windisch, S. Schoberth, S. Meinschmidt, P. Kiesel, A. Knobloch, P. Heremans, B. Dutta, G. Borghs, and G. H. Dohler, "Light propagation through textured surfaces," *J. Opt. A: Pure Appl. Opt.* **1**, 512 (1999).
- ¹⁶R. Windisch, M. Kuijk, B. Dutta, A. Knobloch, P. Kiesel, G. H. Dohler, G. Borghs, and P. L. Heremans, "Nonresonant-cavity light-emitting diodes," *Proc. SPIE* **3938**, 70–76 (2000).
- ¹⁷A. David, "Surface-roughened light-emitting diodes: An accurate model," *J. Disp. Technol.* **9**, 301–316 (2013).
- ¹⁸H. Benisty, R. Stanley, and M. Mayer, "Method of source terms for dipole emission modification in modes of arbitrary planar structures," *J. Opt. Soc. Am. A* **15**, 1192–1201 (1998).
- ¹⁹E. Yablonovitch, "Statistical ray optics," *J. Opt. Soc. Am.* **72**, 899–907 (1982).
- ²⁰M. J. Cich, R. I. Aldaz, A. Chakraborty, A. David, M. J. Grundmann, A. Tyagi, M. Zhang, F. M. Steranka, and M. R. Krames, "Bulk GaN based violet light-emitting diodes with high efficiency at very high current density," *Appl. Phys. Lett.* **101**, 223509 (2012).
- ²¹This leads to 8 LED designs; however one was lost during the fabrication process leading to only 7 final designs.
- ²²With the provision that C_{ex} may depend on η to second order due to photon recycling.
- ²³H. De Neve, J. Blondelle, P. Van Daele, P. Demeester, R. Baets, and G. Borghs, "Recycling of guided mode light emission in planar microcavity light emitting diodes," *Appl. Phys. Lett.* **70**, 799–801 (1997).
- ²⁴D. L. Becerra, Y. Zhao, S. H. Oh, C. D. Pynn, K. Fujito, S. P. DenBaars, and S. Nakamura, "High-power low-droop violet semipolar (30-3-1)

- InGaN/GaN light-emitting diodes with thick active layer design,” *Appl. Phys. Lett.* **105**, 171106 (2014).
- ²⁵M. Boroditsky, I. Gontijo, M. Jackson, R. Vrijen, E. Yablonovitch, T. Krauss, C. C. Cheng, A. Scherer, R. Bhat, and M. Krames, “Surface recombination measurements on III-V candidate materials for nanostructure light-emitting diodes,” *J. Appl. Phys.* **87**, 3497–3504 (2000).
- ²⁶A. Getty, E. Matioli, M. Iza, C. Weisbuch, and J. S. Speck, “Electroluminescent measurement of the internal quantum efficiency of light emitting diodes,” *Appl. Phys. Lett.* **94**, 181102 (2009).
- ²⁷C. A. Hurni, A. David, M. J. Cich, R. I. Aldaz, B. C. Ellis, K. Huang, A. Tyagi, R. A. Delille, M. D. Craven, F. M. Steranka, and M. R. Krames, “Bulk GaN flip-chip violet light-emitting diodes with optimized efficiency for high power operation,” *Appl. Phys Lett.* (submitted).